



STUDY ON MECHANICAL PROPERTIES OF REINFORCED CONCRETE EXTERIOR BEAM-COLUMN JOINT UNDER DYNAMIC LOADING

Tsutomu OGAWA¹, Mitsukazu NAKANISHI², Hiromi ADACHI³

SUMMARY

On the basis of the results of previously conducted dynamic and static loading tests [1–4] on reinforced concrete exterior beam-column joints, this paper describes the effects of the loading rate, variable axial force and the anchoring method for main beam reinforcement on the mechanical properties of exterior beam-column joints. Principal conclusions drawn from the study of the test results are as follows:

- (1) Under dynamic loading, material strength increased because of increases in the material strain rate, and the maximum strength of the test specimen increased.
- (2) Increases in concrete strength due to increases in the strain rate caused increases in joint shear capacity that are greater than increases in the flexural strength at the column and beam ends so as to change the mode of failure of the test specimen.
- (3) In cases where joint shear capacity is not sufficiently large, variable axial force in the column could cause local failure in the joint region.
- (4) Under fluctuating axial force conditions, the test specimen underwent the maximum strength under compressive axial force, and the rate of post-peak strength reduction was high.
- (5) In cases where the joint shear capacity of the test specimens used was not sufficiently high, the test specimens showed different modes of failure depending on the anchoring method for main beam reinforcement (U-shaped anchorage or mechanical anchorage). In the test specimens with mechanical anchorage, cracks occurred along the main reinforcing bars in the outer layer of the column.

¹ Dept. of Oceanic Architecture & Engineering, college of Science & Technology, Nihon University, Tokyo, Japan. Email: d043001@edu.cst.nihon-u.ac.jp

² College of Science and Technology, Nihon University, Tokyo, Japan. Email: adachi@ocean.cst.nihon-u.ac.jp

³ College of Science and Technology, Nihon University, Tokyo, Japan. Email: sanwa@ocean.cst.nihon-u.ac.jp

INTRODUCTION

Many cases of earthquake-induced damage to the columns and beams of reinforced concrete structures have been reported in Japan, but not many cases of beam–column joint damage have been reported so far. It has been pointed out, however, that as high-strength concrete and reinforcing bars have come into widespread use in recent years, the cross sections of structural members have become smaller so that the relative strength of joints in structural frames decreases. Consequently, joint design requirements began to be incorporated into seismic design standards. After the Hyogo-ken Nanbu Earthquake of 1995, a number of reports came in of damaged joints in relatively new reinforced concrete structures. As a result, it began to be pointed out that in designing a reinforced concrete building, it is important to determine the failure behavior of beam–column joints, which greatly affects the deformation capacity of the entire structure under earthquake loading and evaluate in detail the degree of joint damage in different limit states.

It was under this background that the authors conducted dynamic and static loading tests of lower-floor exterior beam-column joints of high-rise reinforced concrete structures to investigate the behavior of buildings under earthquake loading [1–4]. Figure 1 shows the scopes of the different tests conducted in different years. In fiscal 1995, 1997, 1998 and 2001, the authors conducted a set of static and dynamic tests on exterior beam-column joint specimens. In 1995 the authors carried out tests involving constant axial force and mechanical anchoring and in 1997 conducted tests involving constant axial force and U-shaped anchoring. In the tests conducted in 1998, different types and levels of forces ranging from high axial compressive force to tensile axial force were applied to column specimens reinforced with U-shape anchored bars. In the tests conducted in 2001, test specimens reinforced with mechanically anchored bars were subjected to variable axial forces.

The purpose of this study is to investigate in detail, on the basis of the results of the tests mentioned above, the effects of different test parameters (loading rate, anchoring method for main beam reinforcement, variable axial force in column) on the failure behavior, strength and deformation capacity of reinforced concrete exterior beam-column joints.

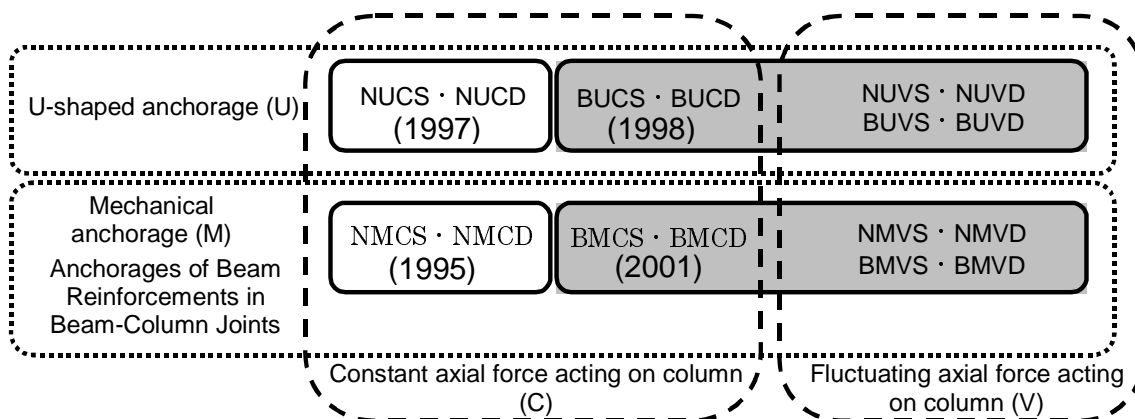


Fig.1 The scopes of the tests conducted in connection with the present study

TESTS

Test specimens

Table 1 lists the test specimens used. Figure 2 shows the test specimen configuration and an example of bar arrangement. Tables 2 and 3 show the material strength of the reinforcing bars and concrete used. The test specimens are exterior beam-column joint models mimicking lower-floor beam–outer column connections of a high-rise reinforced concrete building.

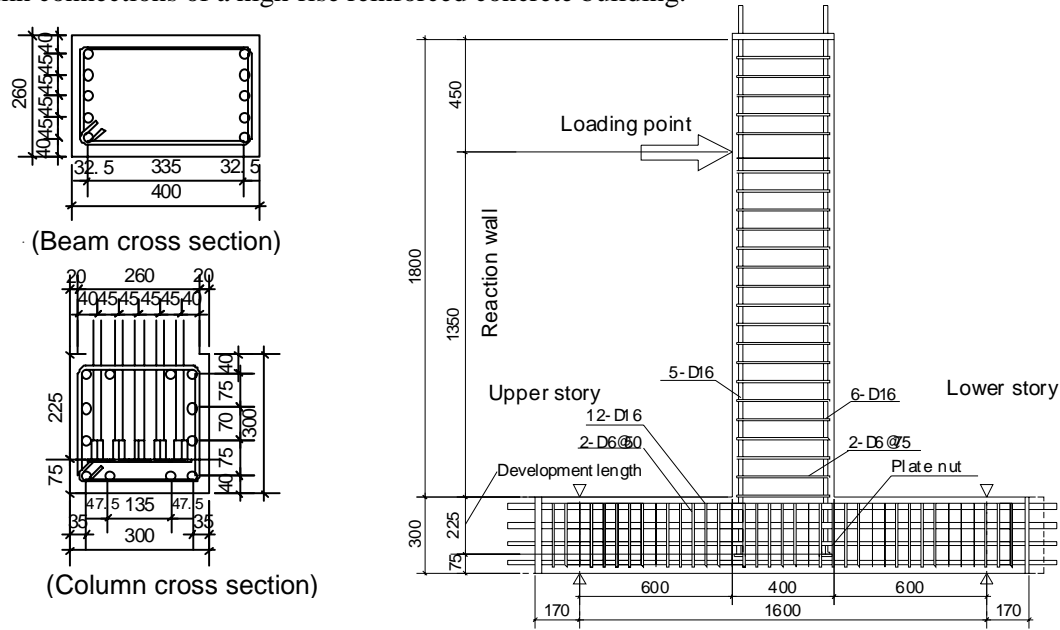


Fig.2 Test specimen configuration and rebar arrangement

Table.1 Test specimens

Name	Year tested	Beam		Column		Joint	Shear–bending capacity ratio	Beam reinforcement anchoring method	Type of axial force applied	Axial force (kN)	Axial force ratio	Loading method
		Main reinforcement	Secondary reinforcement	Main reinforcement	Secondary reinforcement	Secondary reinforcement						
NMCS	1995	6-D16 (SD490)	2-D10@100 (SD295) Pw:0.55%	12-D19 (SD490)	2-D10@75 (SD295) Pw:0.64%	2-D10@75 (SD295) Pwj:0.64%	1.601 (N type)	Mechanical(M)	Constant axial force (C)	150.0	0.05	Static (S)
NMCD							1.601 (N type)	U-shaped(U)				Dynamic(D)
NUCS	1997	6-D16 (SD490)	2-D10@100 (SD295) Pw:0.55%	12-D19 (SD490)	2-D10@75 (SD295) Pw:0.64%	2-D10@75 (SD295) Pwj:0.64%	1.601 (N type)	U-shaped(U)	Constant axial force (C)	150.0	0.05	Static (S)
NUCD							1.601 (N type)	U-shaped(U)				Dynamic(D)
NMVS	2001	6-D16 (SD345)	2-D6@75 (SD295) Pw:0.33%	12-D16 (SD345)	2-D6@50 (SD295) Pw:0.43%	2-D6@50 (SD295) Pwj:0.43%	1.592 (N type)	Mechanical(M)	Fluctuating axial force under earthquake loading (V)	-378.0 ~ 1039.5	-0.20 ~ 0.55	Static (S)
NMVD		10-D13 (SD345)					1.565 (N type)	U-shaped(U)				Dynamic(D)
NUVS	1998	10-D13 (SD345)	2-D6@75 (SD295) Pw:0.33%	12-D16 (SD345)	2-D6@50 (SD295) Pw:0.43%	2-D6@50 (SD295) Pwj:0.43%	1.565 (N type)	U-shaped(U)	Constant axial force (C)	330.8	0.18	Static(S)
NUVD		10-D13 (SD345)					1.565 (N type)	U-shaped(U)				Dynamic(D)
BMCS	2001	6-D16 (SD345)	2-D6@75 (SD295) Pw:0.33%	12-D16 (SD345)	2-D6@50 (SD295) Pw:0.43%	2-D6@50 (SD295) Pwj:0.43%	0.955 (B type)	Mechanical(M)	Sustained constant axial force (C)	330.8	0.18	Static (S)
BMCD		10-D16 (SD345)					1.011 (B type)	U-shaped(U)				Dynamic(D)
BUCS	1998	10-D16 (SD345)	2-D6@75 (SD295) Pw:0.33%	12-D16 (SD345)	2-D6@50 (SD295) Pw:0.43%	2-D6@50 (SD295) Pwj:0.43%	0.955 (B type)	Mechanical(M)	Constant axial force (C)	330.8	0.18	Static(S)
BUCD		10-D16 (SD345)					1.011 (B type)	U-shaped(U)				Dynamic(D)
BMVS	2001	10-D16 (SD345)	2-D6@75 (SD295) Pw:0.33%	12-D16 (SD345)	2-D6@50 (SD295) Pw:0.43%	2-D6@50 (SD295) Pwj:0.43%	0.955 (B type)	Mechanical(M)	Fluctuating axial force under earthquake loading (V)	-378.0 ~ 1039.5	-0.20 ~ 0.55	Static (S)
BMVD		10-D16 (SD345)					1.011 (B type)	U-shaped(U)				Dynamic(D)
BUVS	1998	10-D16 (SD345)	2-D6@75 (SD295) Pw:0.33%	12-D16 (SD345)	2-D6@50 (SD295) Pw:0.43%	2-D6@50 (SD295) Pwj:0.43%	0.955 (B type)	Mechanical(M)	Constant axial force (C)	330.8	0.18	Static (S)
BUVD		10-D16 (SD345)					1.011 (B type)	U-shaped(U)				Dynamic(D)

NMCS

(Shear–bending capacity ratio of joint zone)
N: High
B: Low

(Beam reinforcement anchoring method)
M: mechanical anchorage
U: U-shaped anchorage

(Axial force)
C: sustained constant axial force
V: Fluctuating axial force under earthquake loading

(Loading method)
D: dynamic loading
S: static loading

Table.2 Material strength of reinforcing bars

Year tested	Designation	Standard	Location of use	Yield strength (N/mm ²)	Tensile strength (N/mm ²)
1995	D19	SD490	Main reinforcement	525	720
	D16	SD345		369	535
	D10	SD295	Secondary reinforcement	330	482
1997	D19	SD490	Main reinforcement	575	787
1998	D16	SD345	Main reinforcement	388	599
	D13	SD345		373	526
	D6	SD295	Secondary reinforcement	402	560
2001	D16	SD345	Main reinforcement	392	591
	D6	SD295	Secondary reinforcement	338	486

Table.3 Material strength of concrete

Year tested	Compressive strength (N/mm ²)
7	32.46
9	41.58
10	19.02
13	25.89

Each specimen was configured and sized as a 1/3-scale model. Each test specimen was subjected to either static or dynamic loading, and a total 16 test specimens (8 pairs) were used. The test parameters were defined four two types of specimens: (1) type N specimens designed to have a high shear–bending capacity ratio so that beam-end flexural yielding occurs first, and (2) type B specimens designed to have a low shear–bending capacity ratio, whose shear capacity and flexural capacity are nearly the same. The test specimens of each type were divided into two groups according to the anchoring method for main beam reinforcement [mechanical anchorage (M) and U-shaped anchorage (U)], and each group was further subdivided into two groups according to the loading method for the column [constant axial force (C) and fluctuating axial force (V)]. To investigate the influence of the loading rate on beam–column connections, loads were applied at different rates in both the dynamic and static loading tests.

Loading method

Figure 3 shows the loading apparatus, and Figure 4 shows the loading schedule for dynamic loading under fluctuating axial force conditions. As shown in (a) of both figures, horizontal force was applied to the beam so that displacement values programmed into the actuator were achieved under automatic control. As shown in (b) of the two figures, column axial force was applied so that preset levels of load were applied by the actuator through a level mechanism under automatic control.

In the tests in which constant axial force was applied to the column, axial force was applied at the sustained constant force level, and then horizontal force was applied to the beam. In the tests where fluctuating axial force was applied to the column, axial force was first applied at the sustained constant axial force level, and then axial force in the column was fluctuated according to the horizontal displacement of the beam. When positive horizontal force was applied to the beam, tensile force was applied axially to the column.

Table 4 and Figure 5 show the assumptions made to determine column axial force. In the tests in which fluctuating axial force was applied to the column, the amount of axial force to be applied was determined from the amount of controlled displacement of the beam. The imaginary building considered here is a symmetrical structure, and it is assumed that the building vibrates in the first mode and that axial force increases in proportion to story shear. It is also assumed that the absolute values of axial forces in the right and left outer columns are equal.

In determining the loading rates in the dynamic loading tests, it was assumed, according to the earthquake response analyses of lumped mass systems reported in References 5 and 6, that the maximum displacement rate of the structure was 10 kine, and the maximum displacement rate of the beam was determined accordingly. In the static loading tests, the loading rates were reduced to 1/200 in accordance with the loading schedule used for the dynamic loading. The basic loading method used in both dynamic and static loading tests was to continue cyclic loading until a member rotation angle of 1/25 was reached.

For test specimens that had not lost part of their strength in the static loading tests, loading was continued until a rotation angle of 1/12 was reached.

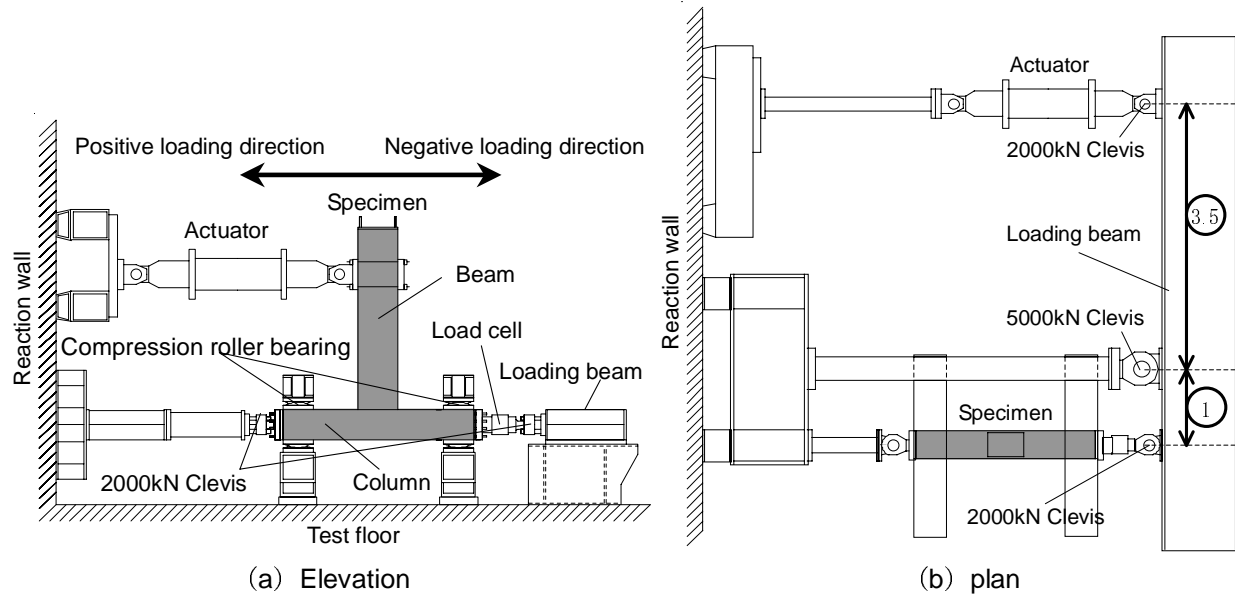


Fig.3 Loading apparatus

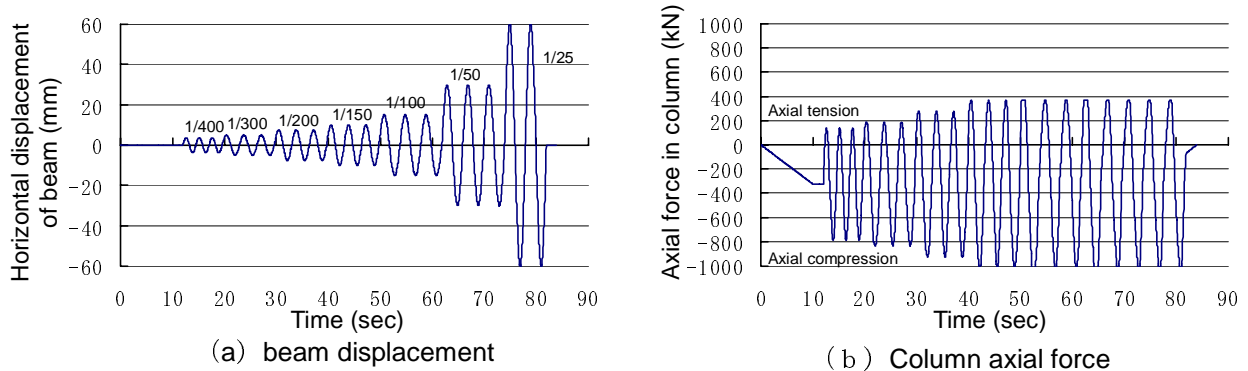
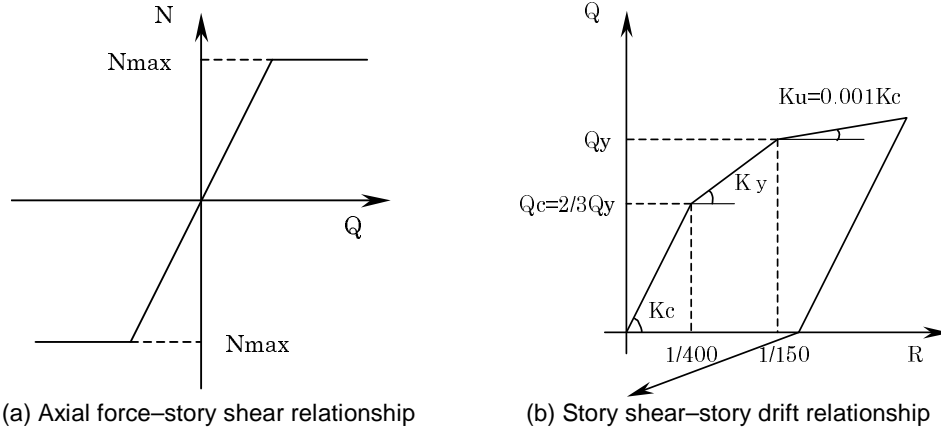


Fig.4 Loading schedule for dynamic loading

Table.4 Basic assumptions for determination of column axial force

1	The building is vibrating in the first mode, and axial force varies in proportion to story shear. The absolute values of the amount of change in axial force in the right-side and left-side outer columns are equal (Figure 5-a).
2	Total collapse of the building occurs at story drift angles of all stories of $R=150$. When this occurs, the drift angle of all stories is 1/150. The amount of change in axial force per story is maximized at a story drift angle of 1/150.
3	Story shear–story drift relationship for a story can be expressed by the Takeda model (Figure 5-b).
4	The maximum axial compression and the maximum axial tension are 0.55 and -0.2 in terms of the axial force ratio.



Q: story shear R: story drift angle N: axial force Q_c : crack strength Q_y : yield strength
 K_c : first stiffness K_y : second stiffness K_u : third stiffness
 N_{max} : maximum value of fluctuating axial compression under earthquake loading
 N_{min} : maximum value of fluctuating axial tension under earthquake loading

Fig.5 Basic assumptions for determination of column axial force

TEST RESULTS

Load–Deformation Relationship

Figure 6 compares load–deformation curves for the static and dynamic loading test results for different test specimens. Comparison of the static loading and dynamic loading test results reveals that for all test specimens, maximum strength under dynamic loading is greater than that under static loading. The effect of dynamic loading on maximum strength is more clearly indicated by type B specimens than by type A specimens. Comparison of the effect of axial force in the column in relation to the shear–bending capacity ratio reveals that type N specimens, whose strength is determined by yielding of the main beam reinforcement,

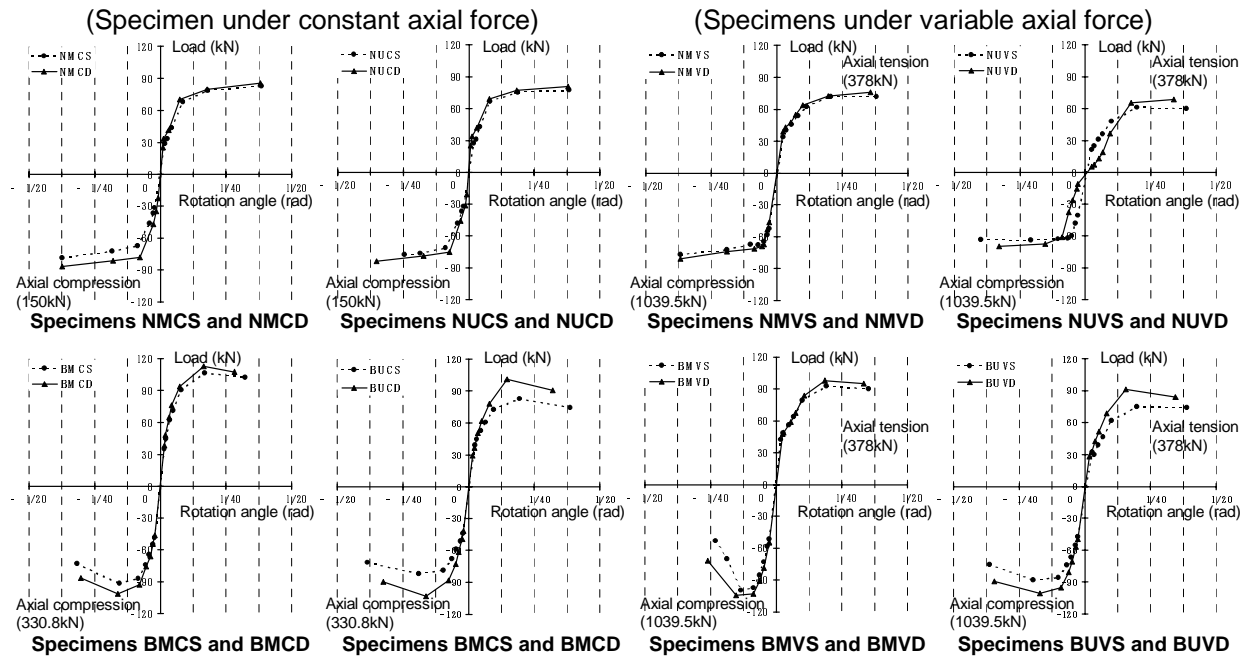


Fig.6 Load–deformation curves

Including the specimens whose columns are subjected to fluctuating axial force, show hysteresis curves similar to those observed under constant axial force conditions, thus indicating little effect of axial force.

Even at a member rotation angle of 1/25, none of the test specimens showed reduction in strength. The reason for this is that even after the beam-end main reinforcement yielded, the joint remained sound enough to resist the fluctuating axial force in the column so that rapid strength reduction was prevented.

In the case of type B specimens, whose joint shear strength and beam flexural strength are nearly equal, maximum strength under fluctuating axial force conditions becomes greater under compressive axial force than under tensile axial force, thus showing differences depending on the type of working axial force. Post-peak strength reduction is slow under tensile axial force is slow, while it is fast under compressive axial force. Type B specimens show greater influence of axial forces than type N specimens.

Maximum strength

Strain rate calculation and increases in material strength

Figure 7 illustrates the method for calculating the strain rate by using a steel strain time history obtained from the dynamic loading tests. For axial steel strains in beam-end main reinforcement (top reinforcement, bottom reinforcement), the strain rate is calculated by dividing the amount of change ($\Delta\epsilon$) occurring during a measurement interval by the measurement interval (Δt : 1/100 s).

The concrete strain rate was assumed to be nearly equal to the strain rate in the main beam reinforcement on the compression side. The maximum strain rates thus obtained were substituted in the material strength increase formulas (1) and (2) shown below, and the values obtained were taken as the material strengths of the reinforcement and the concrete under dynamic loading. Table 5 shows the maximum strain rates of different test specimens and the percentages of material strength increase obtained from the formulas (1) and (2).

The experimentally determined maximum strain rates ranged from about 10^{-3} to 10^{-1} (sec^{-1}) for the reinforcement and from about 10^{-3} to 10^{-2} (sec^{-1}) for the concrete. These values show agreement with the range of strain rates that are thought to be experienced by buildings during earthquakes [7]. This indicates that the values shown above are fairly accurate. The yield point strengths of reinforcement and concrete obtained from these strain rates increase by about 8 to 16% and 19 to 25%, respectively.

(Material strength increase formulas)

Reinforcement

$$D_{fy} / S_{fy} = 1.2 + 0.05 \log \dot{\epsilon} \quad \dots(1)$$

Concrete

$$D_{FC} / S_{FC} = 1.38 + 0.08 \log \dot{\epsilon} \quad \dots(2)$$

$\dot{\epsilon}$: strain rate (1/sec)

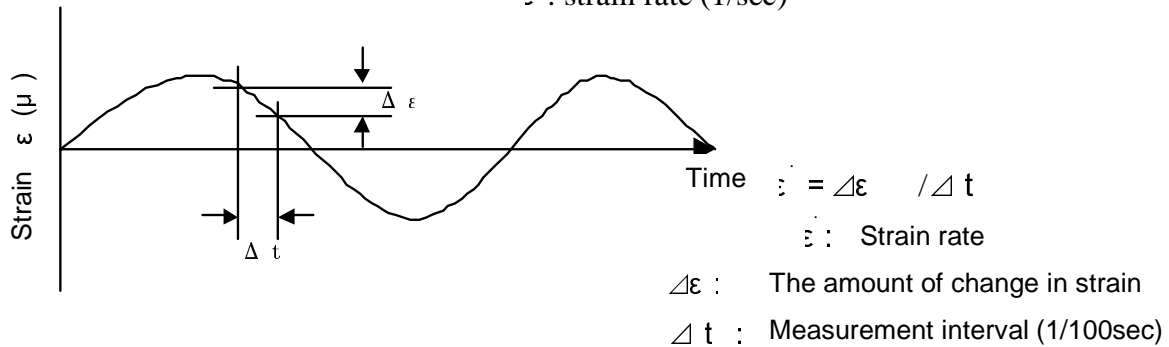


Fig.7 Method for calculating the steel strain rate

Table.5 The maximum strain rate and the percentage of increase in material strength under dynamic loading

Year tested		1995	1997	1998			2001	
Specimen		NMCD	NUCD	NUVD	BUCD	BUVD	BMCD	BMVD
Strain rate (1/sec)	Reinforcement	0.135	0.0374	0.0871	0.005	0.0044	0.121	0.178
	Concrete	0.0254	0.0187	0.006	0.0045	0.0052	0.008	0.008
Percentage of increase in material strength(%)	Reinforcement	10.64	12.86	14.70	8.47	8.21	15.41	16.25
	Concrete	25.24	24.17	20.21	19.21	19.75	21.22	21.22

Measured maximum strength and the percentage of increase in maximum strength

Table 6 compares measured maximum strengths of the test specimens subjected to static loading and dynamic loading with calculated values obtained from strength formulas [8]. The table also shows the percentages of material strength increase under dynamic loading, along with shear–bending capacity ratios and the modes of failure. The calculated values of ultimate strength indicate loads at the loading point on the beam at different breaking strengths. The calculated values for dynamic loading were obtained by using the dynamic material strength values obtained in the preceding section. The percentage of material strength increase under dynamic loading indicates the percentage of material strength increase from the maximum strength under static loading.

In all test specimens except in the positive loading of the NMC specimens, maximum strength increased by 5 to 25% under the influence of loading rates. Comparison of U-shaped anchorage and mechanical anchorage reveals that the percentages of strength increase of type B specimens with main beam reinforcement anchored by the U-shaped anchorage method tend to be considerably higher than the percentages of increase shown by the specimens with mechanically anchored main beam reinforcement.

Table.6 Measured and calculated values of maximum strength, the shear–bending capacity ratio and the modes of failure

Specimen	Measured maximum strength (kN)		Percentage of strength increase under dynamic loading (%)		Calculated ultimate strength(kN)						Shear–bending capacity ratio	Mode of failure
	Positive loading	Negative loading	Positive loading	Negative loading	Beam flexural	Percentage of increase (%)	Joint shear	Percentage of increase (%)	Bearing pressure	Percentage of increase (%)		
NMCS	91.4	81.4	—	—	81.8	—	121.4	—	115.3	—	1.60	B+CC
NMCD	88.8	91.4	-2.9	12.3	91.1	11.4	142.1	17.1	123.2	6.9	1.70	B+CC
NUCS	77.8	77.3	—	—	81.8	—	121.4	—	—	—	1.60	B+T
NUCD	80.9	83.5	4.6	8.0	92.8	13.4	141.2	16.3	—	—	1.65	B
NMVS	71.8	76.7	—	—	61.0	—	93.1	—	78.0	—	1.62	B
NMVD	75.5	80.6	5.2	5.1	64.8	6.2	106.7	14.6	79.0	1.3	1.65	B
NUVS	60.8	63.6	—	—	58.1	—	72.9	—	—	—	1.27	B
NUVD	68.2	96.4	12.3	9.1	69.0	18.8	92.1	26.3	—	—	1.41	B
BMCS	106.2	91.8	—	—	95.6	—	93.6	—	122.2	—	0.97	B
BMCD	112.5	101.3	6.0	10.4	106.5	11.4	106.5	13.8	131.5	7.6	1.00	B
BUCS	82.8	82.0	—	—	94.6	—	72.9	—	—	—	0.78	J
BUCD	100.5	102.9	21.4	25.4	104.0	9.9	91.6	25.7	—	—	0.90	BJ
BMVS	93.0	99.5	—	—	95.6	—	83.6	—	122.2	—	0.97	JB
BMVD	98.0	104.3	5.4	4.8	105.0	9.8	106.1	26.9	131.3	7.4	1.01	JB
BUVS	94.0	88.0	—	—	94.6	—	72.9	—	—	—	0.78	JB
BUVD	91.1	100.8	22.5	14.6	103.8	9.7	91.9	26.1	—	—	0.91	BJ

(Modes of failure)

B: bending failure of beam **J:** Joint shear failure

BJ: flexural yielding of beam followed by joint shear failure

JB: bending failure of beam occurring almost simultaneously with joint shear failure

T: lateral splitting failure **CC:** punching shears failure

Relationship between the increase in shear–bending capacity ratio due to the loading rate and the mode of failure

Comparison of the calculated ultimate strengths of different test specimens shown in Table 6 reveals that the percentages of increase in flexural strength of the beam and the percentages of increase in joint shear strength are 6 to 19% and 14 to 27%, respectively. The reason why the percentages of increase in joint shear strength are higher is that because the percentages of increase in reinforcement strength were higher than the percentages of increase in concrete strength as can be seen from the comparison of the percentages of increase in material strength shown in Table 5, the percentages of increase in joint shear strength were higher than the percentages of increase in flexural strength. This indicates that the shear–bending capacity ratio of the joint increases under the influence of the loading rate.

A look at the effect of increase in the shear–bending capacity ratio on the mode of failure reveals that the NMC specimens underwent punching shear failure in both the static and dynamic loading tests. All the other type N specimens underwent bending failure of the beam and did not show the influence of the loading rate.

In the case of type B specimens with main beam reinforcement anchored by the U-shaped anchorage method, joint shear failure occurred under static loading, but dynamic loading tended to induce a mode of failure accompanied by bending failure of the beam or yielding of the main beam reinforcement. This is thought to be because the percentage of increase in shear strength is higher than the percentage of increase in flexural strength caused by the loading rate. The test specimens with mechanically anchored main beam reinforcement did not show the influence of the loading rate even though the shear–bending capacity ratio at the joint rose.

These results indicate that increases in material strength due to increases in the loading rate could not only increase the strength of building members but also alter the mode of failure of beam–column joints.

Final failure condition

Effects of dynamic loading

Figure 8 shows the final failure conditions. Type N specimens both under static loading and under dynamic loading are characterized by severe beam-end damage. Under dynamic loading, the number of cracks is relatively small and joint failure is slight. Type B specimens both under static loading and dynamic loading are characterized by severe joint damage. Under dynamic loading, joint damage tends to be less severe, the crack zone tends to be smaller, and failure phenomena tend to be more concentrated than under static loading.

Effects of fluctuating axial force in column

Type N specimens underwent local (beam end) flexural failure, regardless of the type of working axial force. Type N specimens subjected to fluctuating axial force were characterized by extensive cracks on the right and left sides of the column.

Type B specimens subjected to fluctuating axial force were characterized by major cracking on the right and left sides of the column and the outer side of the column and tended to suffer damage at the joint.

Effects of the anchoring method for main beam reinforcement

Comparison was made between the mechanical anchorage method and the U-shaped anchorage method used for type B specimens. In the specimens with mechanically anchored main beam reinforcement, diagonal cracks occurred at the joint and major cracking occurred on the outer side of the column along the main reinforcement.

Comparison of the test specimens subjected to fluctuating axial force under dynamic loading (BMVD, BUVD, NMVD, NUVD) shows that NUVD suffered least joint damage and underwent beam flexural failure. BMVD suffered the severest joint damage and underwent local joint failure.

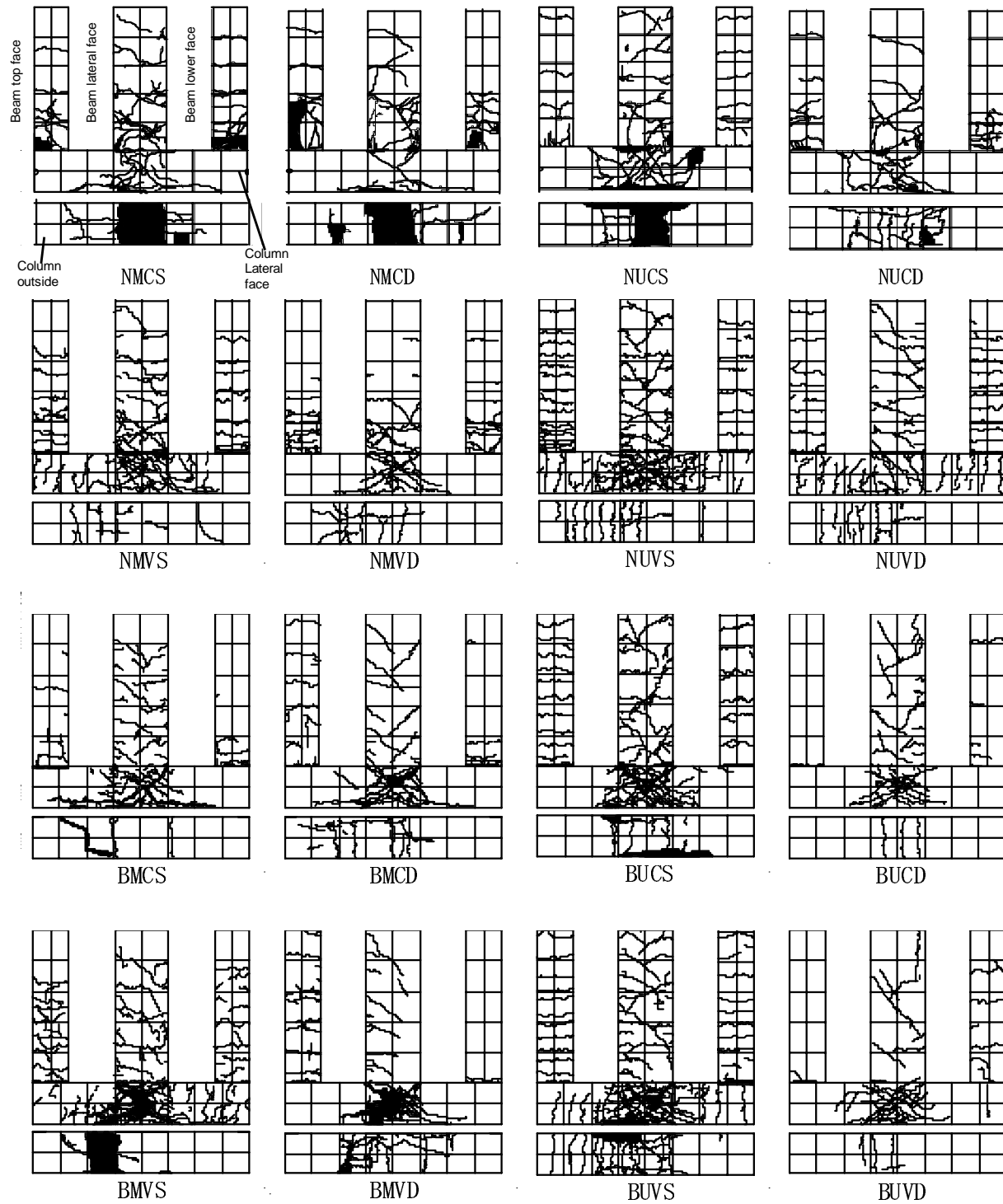


Fig.8 Final failure conditions

Identification of deformation components

Figure 9 illustrates the concept of measured displacement. In displacement measurement, stroke-type displacement meters were used to measure beam displacement (X1), joint rotation (X2, X3), vertical displacement of the joint zone (X4, X5), horizontal displacement of the joint zone (X6, X7) and diagonal displacement of the joint zone (X8, X9). Figure 10 shows the method for calculating the shear deformation angle of the joint zone.

In order to investigate the effects of the loading rate and working axial force on the beam, the column and the joint zone, their deformation components were converted to the amounts of deformation at the loading point, by using the equations shown in Figures 9 and 10, and compared. Figure 11 shows the load–deformation relationships for different deformation components of the beam during the loading process, which was terminated when the member rotation angle reached 1/50.

Comparison of the hysteresis loops for static loading and dynamic loading reveals that the deformation components of the type N specimens under static loading and dynamic loading show similar tendencies. In the case of the type B specimens, however, the maximum deformation of the joint component becomes smaller under dynamic loading.

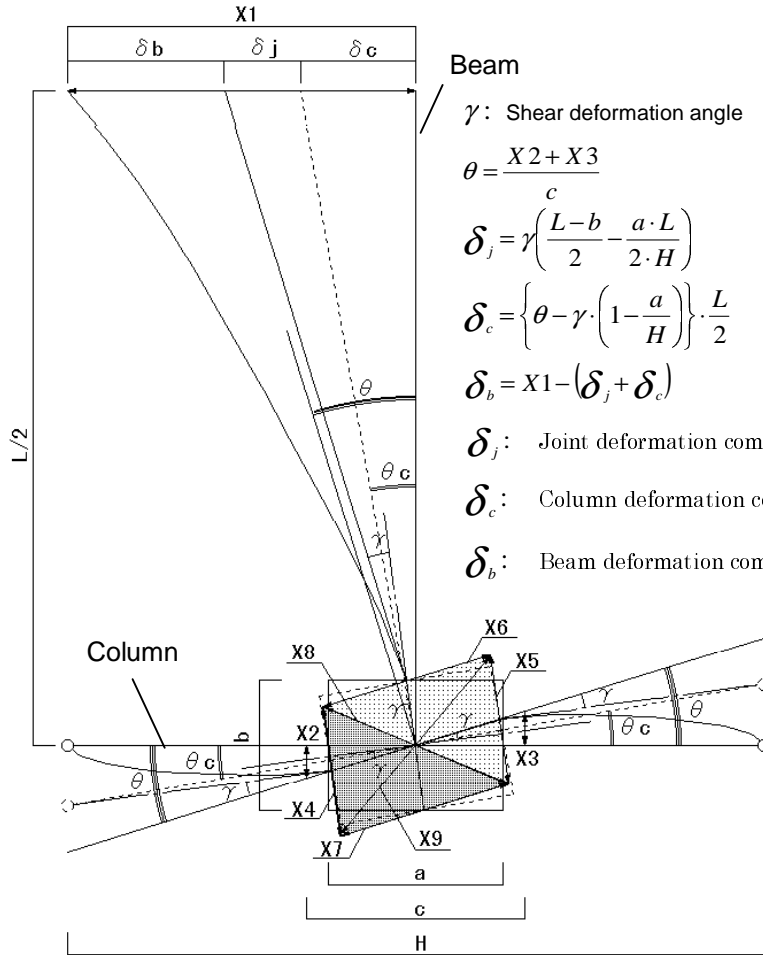


Fig.9 Concept of measured displacement

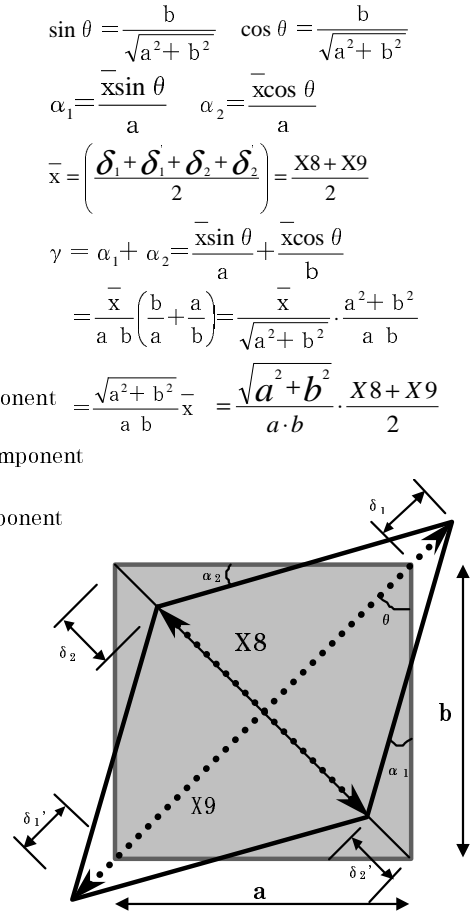


Fig.10 Calculation of the shear deformation angle of the joint zone

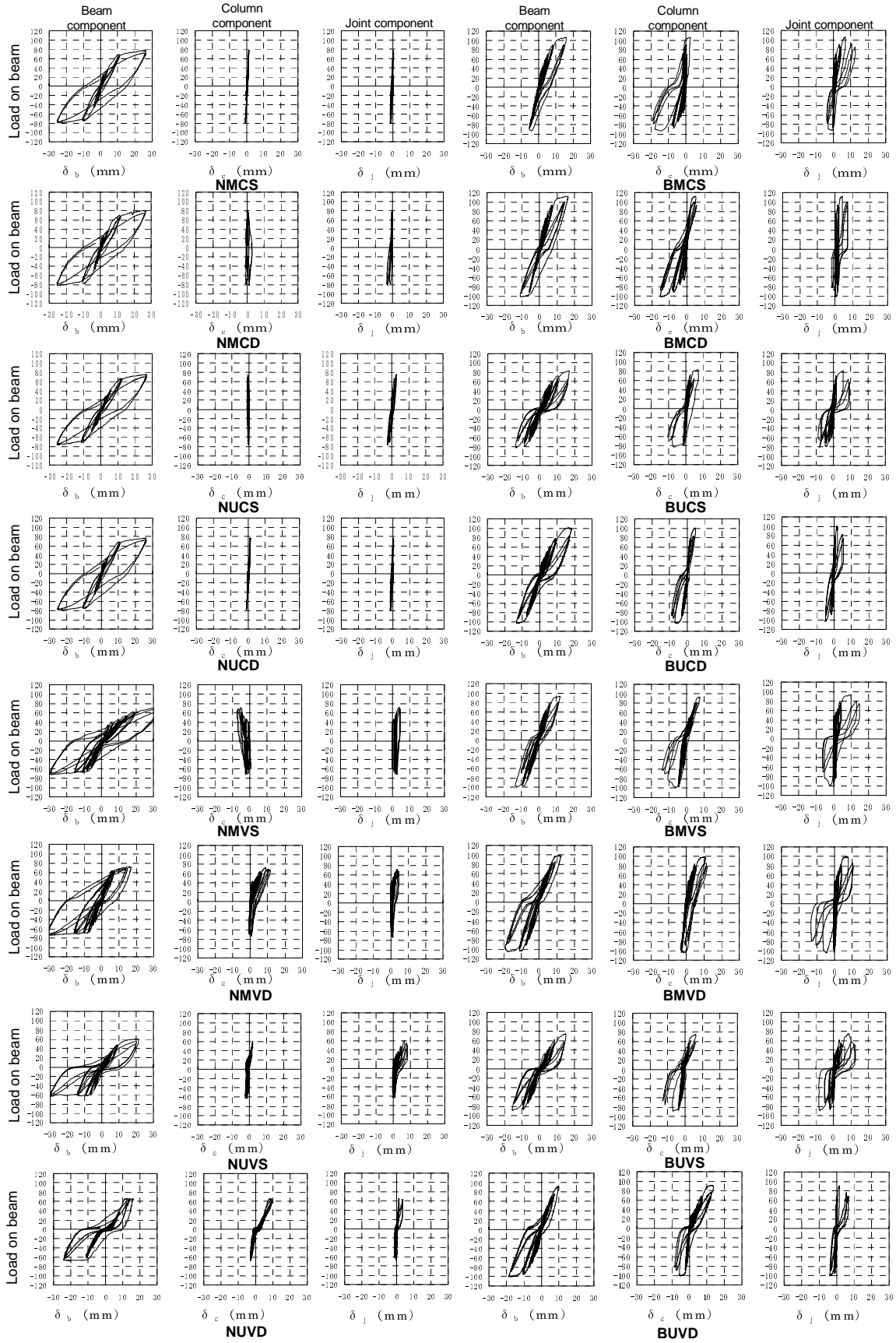


Fig.11 Identification of load–deformation curve components (rotation angle: 1/400 to 1/50)

Comparison in terms of the shear–bending capacity ratio reveals that the type N specimens are characterized by spindle-shaped hysteresis loops for the beam component, and that the amounts of deformation of the column and joint components are smaller than those of the beam component. The type B specimens show inverted-S-shaped hysteresis loops for the beam component. Unlike the type N specimens, the type B specimens show considerable increases in the amount of deformation of the column and joint components.

Examination of the effects of axial force in the column reveals that under variable axial force, the amount of deformation in the positive loading (axial tension) of the beam component tends to decrease, while the amount of deformation in negative loading (axial compression) tends to increase.

In the case of the column and joint components, the amount of deformation in the positive loading (axial tension) of the type N specimens becomes greater than under constant axial force as the load acting on the beam increases. On the negative loading side (axial compression side), however, the deformation of the column and the joint zone does not increase as the amount of beam deformation increases. In the case of the type B specimens, the joint zone component tends to show a conspicuous inverted-S-shaped slip pattern.

CONCLUSIONS

- (1) Under dynamic loading, as the material strain rate increased, material strength increased so that the maximum strength of the specimen increased.
- (2) Increases in concrete strength due to increases in the strain rate altered the mode of failure of the test specimen because the shear capacity of the joint zone was increased more than the column and beam-end flexural strength.
- (3) In cases where fluctuating axial force acts on the column, local failure of the joint zone could occur if the shear–bending capacity ratio of the joint is small.
- (4) Under variable axial force, the test specimens underwent maximum strength when subjected to axial compression, and lost its strength sharply after the maximum strength was reached.
- (5) In the case of test specimens whose joints had a low shear–bending capacity ratio, the mode of failure varied depending on the anchoring method for main beam reinforcement. In the test specimens with mechanically anchored main beam reinforcement, major cracking occurred along the main column reinforcement on the outer side of the column.

ACKNOWLEDGMENT

This study was conducted as part of the Study on Environmentally Sustainable and Disaster-resistant Cities (leader: Iwao Otsu, Director, Research Institute of Science and Technology; committee chairman: Shinji Ishimaru) undertaken under the "Academic Frontier Promotion Program (College of Science and Technology, Nihon University) of the Ministry of Education, Culture, Sports, Science and Technology. The authors would like to thank all the people concerned.

REFERENCES

1. Adachi, H. Okuda, A. et al. "Experimental Study on Effect of Loading Rate on Mechanical Properties of R/C External Beam-Column Joints with Mechanical Anchorages." Proceedings of the Japan Concrete Institute , Vol.18, No.2, pp.971~976, 1996 .

2. Adachi, H. Masujima, K. et al. "Experimental Study on Effect of Loading Rate on Mechanical Properties of R/C External Beam-Column Joints." Proceedings of the Japan Concrete Institute , Vol.20, No.3, pp.553~558, 1998 .
3. Adachi, H. Yamada, T. et al. "Experimental Study on Mechanical Properties of R/C Exterior Beam-Column Joint under Fluctuating Axial force." Proceedings of the Japan Concrete Institute , Vol.21, No.3, pp.637~642, 1999 .
4. Adachi, H. Kojima, Y. et al. "Experimental Study on of R/C Exterior Beam-Column Joint with Mechanical Anchorages under Fluctuating Axial force." Proceedings of the Japan Concrete Institute , Vol.24, No.2, pp.445~450, 2002.
5. Hosoya, H. Abe, I. et al. "A Study of the Effect of Strain Rate on Strength and Mode of Failure of Reinforced Concrete (RC) Members-Material Tests and Horizontal Loading Tests of Column Members under the High Axial force-" Concrete Research and Technology, Vol.4, No.2, pp.43~55, July.1993.
6. Hosoya, H. Abe, I. et al. "A Study of the Effect of Strain Rate on Strength and Mode of Failure of Reinforced Concrete (RC) Members-Static and Dynamic Horizontal Loading Tests of Column Members for Shear Failure-"Concrete Research and Technology, Vol.5, No.1, pp.39~49, Jan.1994.
7. Otani, S. "Influence of Loading Rate on Behavior of Reinforced Concrete." Concrete Journal, Vol.21, No.11, pp.23~34, Nov. 1983.
8. Architectural Institute of Japan. "Design Guideline for Earthquake Resistant Reinforced Concrete Buildings Based on Inelastic Displacement Concept."1999.